A Numerical Modeling of Heat and Mass Transfer for a Falling Film Absorber

Hamza M. Habib[1] , Ahmed M. Ebady[2] , Essam R. El-Zahar[3]

Department of Mathematics, College of Sciences and Humanities,
Sattam Bin Abdulaziz University, Alkharj, KSA.

Abstract

A numerical model of combined heat and mass transfer in the two-phase flow occurring during the absorption of a water vapor into a falling film of LiBr-H2O is presented. A thin liquid film flows downward over an isothermal wall of a vertical channel while water vapor is pumped between the liquid free surface and the other adiabatic wall of the channel. Fluid properties are considered variables. It was found that the absorption rate increases strongly by increasing the absorber water vapor pressure, the inlet solution concentration, or by lowering the isothermal wall temperature. The inlet solution temperature affects the entrance region only. The numerical results are in agreement with the available experimental data.

Keywords: Thin film flow, Absorption, Aqueous lithium bromide

NOMENCLATURE :

C	absorbent concentration in weight fraction of salt
C_p	Specific heat, kj/(kg °C)
D	Diffusion coefficient , m^2/s
H_a	heat of absorption, kj/kg
k	conductivity, kj/(m s °C)
P	Water vapor pressure, mm-Hg
Re	Reynolds Number
T	temperature, °C
u	velocity in transverse direction, m/s
v	velocity in streamwise direction, m/s

Greek Letters

δ	film thickness, m
μ	viscosity, $kg/(m^3 \ s)$
ρ	density, kg/m^3

Subscript

g	Water vapor
ℓ	Liquid
0	Inlet
n	Interface

INTRODUCTION

Absorption of gases into thin films is used widely in modern applications of heating and refrigeration systems such as chillers, absorption air-conditioners, or heat pumps, etc. The systems of LiCI-H2O and LiBr-H2O are the most commonly used materials in such applications. The analysis of film absorption is very complicated due to the presence of waves at the free surface of the film, the equilibrium and interfacial relations, the heat generation, and the accumulation of air at the interface.

Theoretical work on film absorption was reported by many researchers. Nakoryakov et al. [1] presented a simple model including a linear temperature and constant velocity profiles. Later in [2] they improved the model by solving the energy equation. Further, in [3] they studied the heat and mass transfer in the entrance region and gave some estimates for the relative lengths for each process. Grossman [4] extended the model used by Nakoryakov [2] to include adiabatic wall boundary condition.

The effect of variable properties and shear stress was studied by Yih and Seagrave [5]. A decrease in film thickness and enhancement in the mass transfer was reported due to the co-current gas stream.

Andberg [6], and Andberg et al. [7] introduced a sophisticated numerical model of film absorption which allows film thickness to vary. They reported several regions to identify the development of the concentration and temperature along the film.

Yang [8] developed a numerical model similar to Andberg [6] except that film thickness is constant. His results agree well with those of (Andberg [6]).

An analytical model for film absorption with varying film thickness is reported by Conlisk [9, 10]. Practically, the mass rate of vapor absorbed is very small compared to the solution

flow rate and the film thickness can be considered constant as reported by Yang [8] .

Nakoryakov et al. [11] used the Fourier transform method in his model. His solution suffered oscillations at the entrance region.   Later in [12] they treated the entrance region separately using a self-similar solution to avoid such oscillations.

Yoon et al. [13] used a numerical model for the absorber. They included the inter-diffusion term in their formulation and allowed the wall temperature to vary linearly. Karami and Farhanieh [14] solved the same problem as Yoon et al. [13]; however, they considered variable properties of the film. They claim that their model could predict absorption rates for Reynolds numbers up to 120. It should be noted that waves dominate the flow regime for Re> 30 (Yang [21]). The model introduced by Bo et al. [15] included variable thermosphysical properties of the film and a convection boundary condition at the wall.

Analytical models using Laplace transform method were reported by Meyer [16, 17] and Mortazavi et al. [18]. Meyer [16, 17] assumed constant velocity profile. And Mortazavi et al [18] constant and linear velocity profiles. They indicated that the mass transfer rates are greater when using the linear velocity profile. Recently, Hosseinnia et al. [19] studied the Soret and Dufour effects. They concluded that these two effects have a little contribution to absorption rate.

Burdukov et al. [20] in his experimental study pointed out a falling film absorber's performance exceeded the performance of a bundle tube finned-absorber. Yang [21], and Ameel [22] reported that experimental results for smooth film are hard to obtain without nonabsorbable gases. Waves appear at small Reynold numbers. Habib et al. [23] showed that the presences of small amount of air reduces the absorption rates significantly. Although the presence of air degrades the absorption rate, the presence of waves enhances it. Within these two effects, the smooth film makes a reasonable choice to model the falling film absorber in the absence of reliable model for wavy film flow.

As it appears from the literature review, past researchers neglected the gas phase to reduce the complexity of the problem. In an effort to improve the modeling of the film absorption, the governing equations for the gas phase and the shear stress at the liquid-gas interface are included. It is also aimed that the model can handle various boundary conditions.

ANALYSIS

The geometry of the absorber chosen for the present application is shown in Fig. 1. A thin liquid film of LiBr-H2O having an initial temperature and concentration of $T_{0\ell}$ and C_0 respectively flows downward over an isothermal wall at T_w of a vertical channel . Water vapor is pumped at the top of the channel at temperature T_{0g} and velocity v_{0g} and

flows between the film surface and the adiabatic wall of the channel. Due to the difference between the water vapor pressure in the two phases an absorption process occurs at the interface. This exothermic process generates heat at the interface and the coupling between the governing equations for heat and mass transfer becomes inevitable. Part of the energy released is transported to the isothermal wall through the film and the other part is transported to the adjacent water vapor.

The absorber of the open-cycle solar absorption refrigeration system works in the limits of $25 < \mathrm{Re}_\ell < 90$ for the falling film, Siebe [24]. This spans the smooth film to wavy laminar film flow region. Yang [21] and Ameel [22] reported a smooth entry length as much as 20% of the total length of the falling film absorber where the absorption rates are higher.
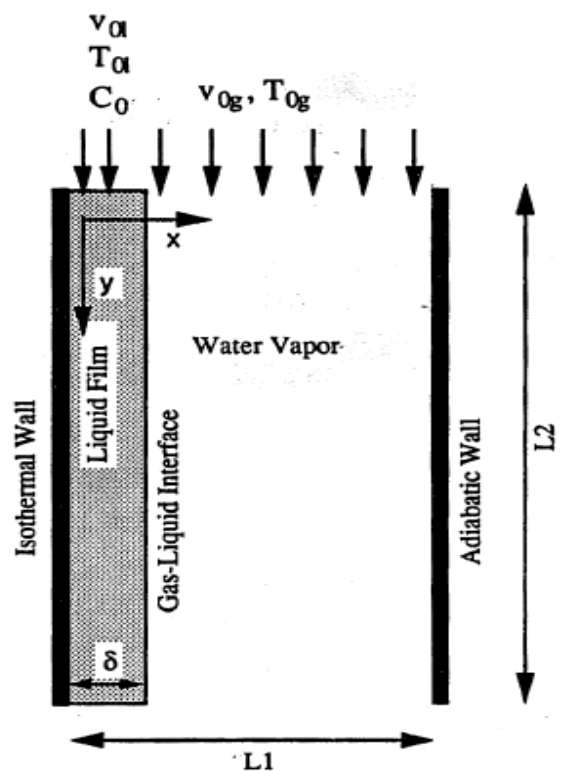

Fig. 1. Schematic of the physical situation

Assumptions:

1. The flow regime is laminar for the liquid and gas phase.

2. The film thickness is constant.

3. Shear stress exists between the two phases (no slip).

4. Fluid properties are variables in both phases.

5. Thermal diffusion and diffusion-thermo effects are insignificant.

6. Thermodynamic equilibrium exists for vapor pressure at the interface.

Governing Equations
a. The Liquid phase

$$\frac{\partial}{\partial x}(\rho_\ell u) + \frac{\partial}{\partial y}(\rho_\ell \upsilon) = 0 \tag{1}$$

$$\rho_\ell u \frac{\partial u}{\partial x} + \rho_\ell \upsilon \frac{\partial u}{\partial y} = -\frac{\partial p}{\partial x} + \frac{\partial}{\partial x}(\mu_\ell \frac{\partial u}{\partial x}) + \frac{\partial}{\partial y}(\mu_\ell \frac{\partial u}{\partial y}) \tag{2}$$

$$\rho_\ell u \frac{\partial \upsilon}{\partial x} + \rho_\ell \upsilon \frac{\partial \upsilon}{\partial y} = -\frac{\partial p}{\partial y} + \frac{\partial}{\partial x}(\mu_\ell \frac{\partial \upsilon}{\partial x}) + \frac{\partial}{\partial y}(\mu_\ell \frac{\partial \upsilon}{\partial y}) + \rho_\ell g \tag{3}$$

$$\rho_\ell c_{p,\ell} u \frac{\partial T}{\partial x} + \rho_\ell c_{p,\ell} \upsilon \frac{\partial T}{\partial y} = \frac{\partial}{\partial x}(k_\ell \frac{\partial T}{\partial x}) + \frac{\partial}{\partial y}(k_\ell \frac{\partial T}{\partial y}) \tag{4}$$

$$\rho_\ell u \frac{\partial C}{\partial x} + \rho_\ell \upsilon \frac{\partial C}{\partial y} = \frac{\partial}{\partial x}(\rho_\ell D_\ell \frac{\partial C}{\partial x}) + \frac{\partial}{\partial y}(\rho_\ell D_\ell \frac{\partial C}{\partial y}) \tag{5}$$

b. The Gas phase

$$\frac{\partial}{\partial x}(\rho_g u) + \frac{\partial}{\partial y}(\rho_g \upsilon) = 0 \tag{6}$$

$$\rho_g u \frac{\partial u}{\partial x} + \rho_g \upsilon \frac{\partial u}{\partial y} = -\frac{\partial p}{\partial x} + \frac{\partial}{\partial x}(\mu_g \frac{\partial u}{\partial x}) + \frac{\partial}{\partial y}(\mu_g \frac{\partial u}{\partial y}) \tag{7}$$

$$\rho_g u \frac{\partial \upsilon}{\partial x} + \rho_g \upsilon \frac{\partial \upsilon}{\partial y} = -\frac{\partial p}{\partial y} + \frac{\partial}{\partial x}(\mu_g \frac{\partial \upsilon}{\partial x}) + \frac{\partial}{\partial y}(\mu_g \frac{\partial \upsilon}{\partial y}) \tag{8}$$

$$\rho_g c_{p,g} u \frac{\partial T}{\partial x} + \rho_g c_{p,g} \upsilon \frac{\partial T}{\partial y} = \frac{\partial}{\partial x}(k_g \frac{\partial T}{\partial x}) + \frac{\partial}{\partial y}(k_g \frac{\partial T}{\partial y}) \tag{9}$$

Boundary and Interfacial Relations

$$\left. \begin{array}{llll} u = 0, \qquad \upsilon = 0 & \text{at } x = 0 & \text{and} & x = L_1 \\ T = T_{0\ell}, \qquad \upsilon = \upsilon_{0\ell}, \quad C = C_0 & \text{at } y = 0 & \text{and} & 0 < x < \delta \\ T = T_{0g}, \qquad \upsilon = \upsilon_{0g}, & \text{at } y = 0 & \text{and} & \delta < x < L_1 \end{array} \right\} \tag{10}$$

$$T = T_w \quad \text{at } x = 0 \tag{11}$$

$$\frac{\partial C}{\partial x} = 0 \quad \text{at } x = 0 \tag{12}$$

$$\frac{\partial T}{\partial x} = 0 \quad \text{at } x = L_1 \tag{13}$$

$$\mu_\ell \frac{\partial \upsilon}{\partial x}\bigg|_{x=\delta} = \mu_g \frac{\partial \upsilon}{\partial x}\bigg|_{x=\delta} \tag{14}$$

$$k_\ell \frac{\partial T}{\partial x}\bigg|_{x=\delta} = k_g \frac{\partial T}{\partial x}\bigg|_{x=\delta} - H_a \rho_\ell D_\ell \frac{\partial C}{\partial x}\bigg|_{x=\delta} \tag{15}$$

$$T_\ell = T_g \quad \text{at } x = \delta \tag{16}$$

$$-\rho_\ell D_\ell \frac{\partial C}{\partial x}\bigg|_{x=\delta} = \rho_\ell u\big|_{x=\delta} \tag{17}$$

$$\frac{\partial u}{\partial y} = 0, \quad \frac{\partial \upsilon}{\partial y} = 0, \quad \frac{\partial T}{\partial y} = 0, \quad \frac{\partial C}{\partial y} = 0 \quad \text{at} \ y = L_2 \tag{18}$$

Finally, the concentration, pressure, and temperature are interrelated to each other through the following equilibrium relation at the liquid-vapor interface.

$$C_n = f(p_n, T_n) \tag{19}$$

The data for LiBr-H2O can be found in McNeely [25].

Siebe [24] gives a convenient correlation for Eq. (19) in the form

$$\log_{10} P = A + B/T + D/T^2 \tag{20}$$

Where

$$\left. \begin{array}{l} A = a_0 + a_1\,C + a_2\,C^2 + a_3\,C^3 \\ B = b_0 + b_1\,C + b_2\,C^2 + b_3\,C^3 \\ D = d_0 + d_1\,C + d_2\,C^2 + d_3\,C^3 \end{array} \right\}$$

The equations are discretized using the control volume formulation as described by Patanker [26]. At the entrance region the boundary conditions are discontinuous in temperature and/or concentration. To deal with the large gradients at the liquid-gas interface, a nonuniform grid in the both directions is adopted. The grid is clustered around the interface from both sides. The solution is considered converged when the maximum relative change in the velocity, temperature and concentration is less than 10^{-6}.

RESULTS AND DISCUSSIONS

To represent the results in a nondimensionalized form is not an easy task. The empirical thermodynamic equilibrium relation Eq. (20) precludes the non-dimensionalization. To get some insight into the absorption process, the code was run for a H2O-LIBr solution with the conditions and operating parameters indicated in Table 1 for a typical operation of the absorber (Siebe [24]).

Table 1: Absorber Conditions and Operating Parameters

Absorber pressure	7.02 mm-Hg
Inlet bulk solution temperature	44.44°C
Inlet bulk solution concentration	60%
Wall temperature	35°C
Inlet water vapor temperature	20°C
film Reynolds number	30
Water vapor Reynolds number	30
Absorber length	1m

The concentration and temperature distributions across the liquid film are given in Fig 2. and Fig 3. respectively. The drop in the interface concentration in the flow direction occurs at a faster rate than the absorption of water vapor is transported through the film. This continuous drop in the interface concentration causes the interface temperature to drop since they are interconnected through the equilibrium relation. Eventually the interface temperature approaches the isothermal wall temperature.

Fig. 2. Concentration distribution of LiBr across the film

Fig. 3. Temperature distribution across the film

Absorption of water vapor releases energy at the interface. Part of this energy is transferred to the gas phase causing its temperature to rise in the flow direction. Figure 4 shows the temperature distribution across the gas at different positions in the streamwise direction. The temperature is higher at the interface and decreases as it approaches the adiabatic wall.

The rise in the gas temperature continues in the streamwise direction.

Figure 5 shows streamwise temperature distribution at the interface and in the bulk of the liquid film. As the flow moves downward the isothermal wall, the interface temperature of LiBr continues to drop because the heat is removed away from the film to the isothermal wall and also to the adjacent water vapor. The bulk temperature of the film follows the drop in the interface temperature. This dropping of interface temperature continues until the bulk and interface temperatures flatten at the temperature of the isothermal wall.
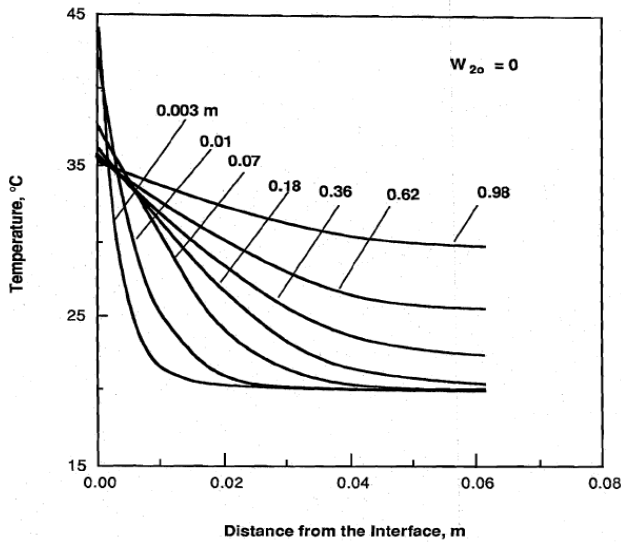
Fig. 4. Temperature distribution across the gas phase at various locations from the inlet
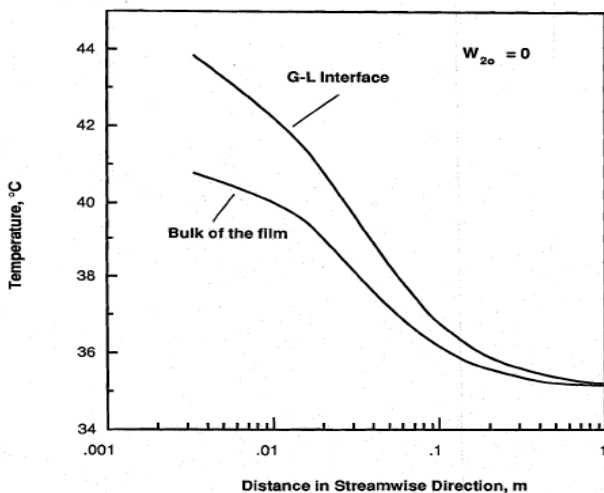
Fig. 5. Streamwise temperature distribution at the interface and in the bulk of the liquid film

The most important aspects of these results are the heat and mass fluxes versus the length. Figure 6 shows the local mass flux absorbed at the interface. Since the initial temperature profile at the interface is elevated and flat, it precludes a large amount of absorption at the interface, Once a temperature gradient through the film is developed it becomes able to

transport the heat of absorption to the isothermal wall through the film. However, since the inlet solution temperature is a few degrees below the equilibrium conditions, a modest amount of absorption may take place immediately, with the heat of absorption going into sensible heating of the surface of the film and the adjacent vapor in the gas phase. Notice that the mass flux is increased because the wall cooling effect propagates out to the interface. The mass flux continues to increase until it reaches a maximum, this is due to the gradual formation of a flat temperature profile in the film. After the initial region, the effects of the interface coupling become apparent. As indicated in Figure 3, the interface temperature drops as the fluid moves downward. This reduces the driving potential for heat and mass transfer within the film.
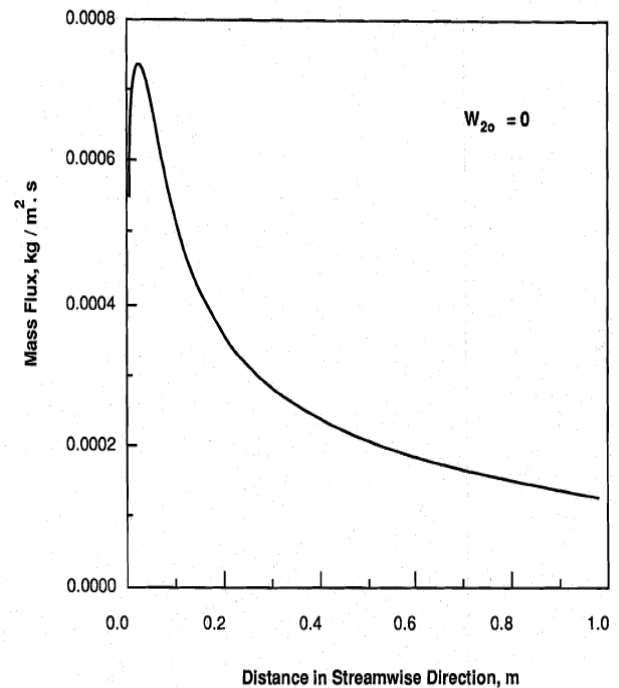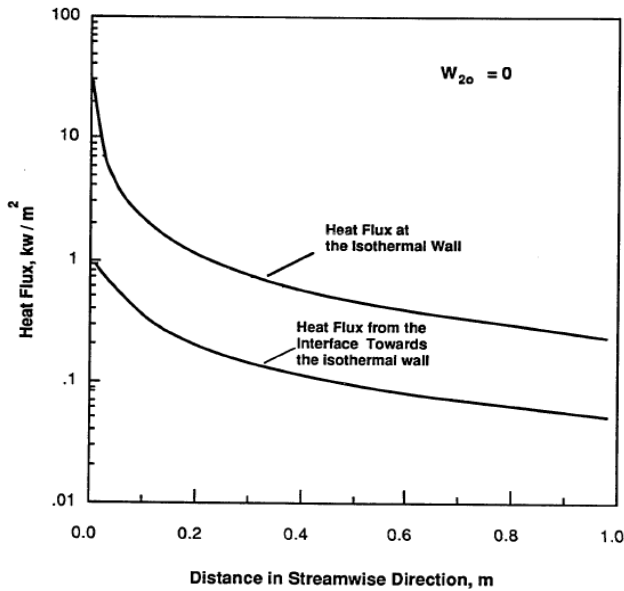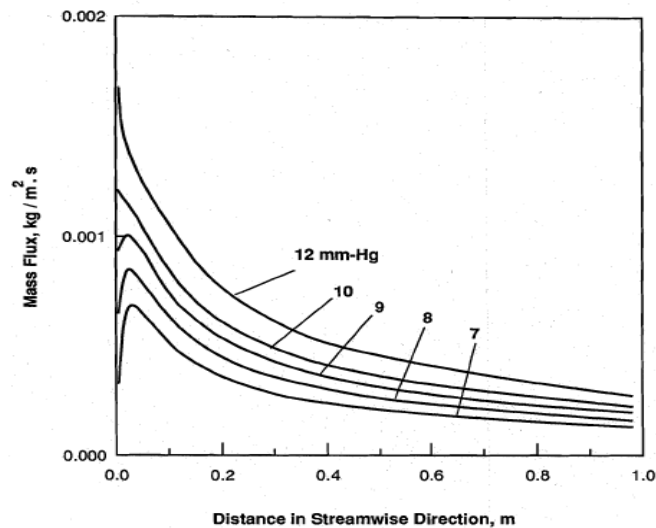

Fig. 6. Local mass flux at the interface

Figure 7 shows the local heat flux directed from the interface towards the isothermal wall and at the isothermal wall at $x = 0$. Near the inlet, the film is at a uniform and elevated temperature with respect to the wall, and the process is dominated by sensible heat in the film. Due to the absorption process, the heat released at the interface causes a gradient in the temperature in both liquid and gas phases. The heat flux through the interface toward the wall decreases in the streamwise direction due to the decrease in the driving forces. At some distance downstream, the values of the heat fluxes at the interface and the wall become very close to each other.

Fig. 7. Local heat flux from the interface towards the
isothermal wall and at the isothermal wall

The driving potential for mass transfer through a liquid-gas interface is the water vapor pressure difference between the two phases. Figure 8 illustrates the effect of the absorber water Vapor pressure on the local mass flux absorbed at the interface. As indicated in Figure 8; a higher absorber pressure results in a higher mass transfer rate. However, the higher absorber pressure yields a higher evaporator temperature that is not favorable to the overall performance of the absorption cycle.

Fig. 8. Effect of the absorber water vapor pressure on the
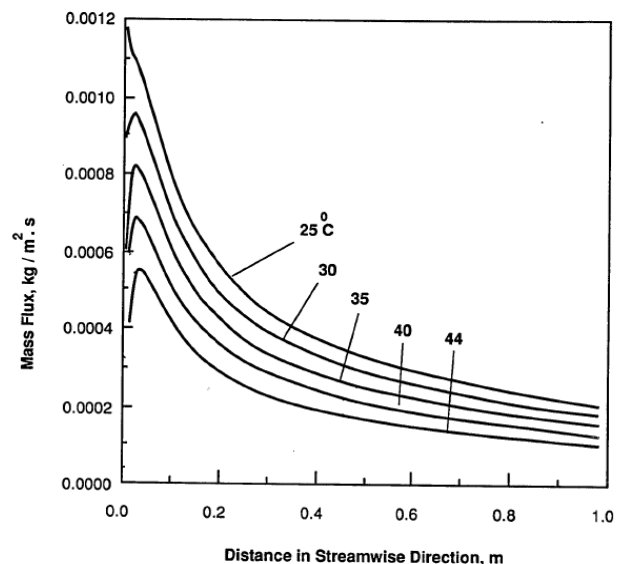absorbed mass flux at the interface

Similar to the effect of absorber vapor pressure, a higher concentration yields a higher driving potential. However, crystallization may occur at higher concentration of LiBr. The

effect of changing the inlet concertation of LiBr is shown in Figure 9.
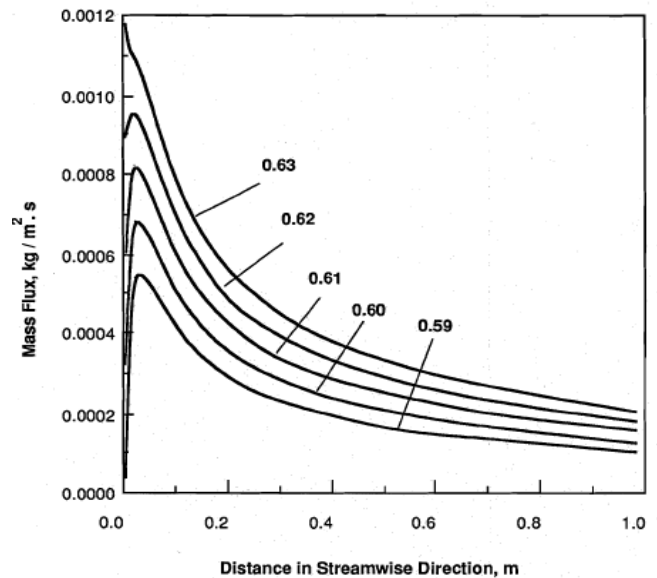
Fig. 9. Effect of the inlet film concentration on the absorbed
mass flux at the interface

In order to maintain the proper mass transfer rate, the heat generated due to absorption process must be removed from the liquid solution. Hence, the wall temperature has an important role in mass transfer. Figure 10 shows the effect of the isothermal wall temperature on the local mass flux of water vapor absorbed at the interface for wall temperatures 25, 30, 35, 40 and 44°C. As indicated in the figure lowering the wall temperature increases the mass transfer rates. In other words, higher wall temperatures have an adverse effect on heat and mass transfer. However, this is limited by the supply water cooling temperature.


Fig. 10. Effect of the isothermal wall temperature on the
absorbed mass flux at the interface

Figure 11 illustrates the effect of inlet solution temperature on the local mass flux absorbed at the interface for inlet solution temperature of 35, 37, 39, 41 and 44°C, respectively. Increasing the inlet solution temperature reduces the initial pressure driving force and thus, degrades the absorption rate. But, there is another factor which to be considered, decreasing the inlet solution temperature below a certain degree will lower the mass diffusivity, because it is mainly dependent on solution temperature. However, the effect of inlet solution temperature dominates the entrance region only and has no significant effect from a design standpoint. That is, the initial temperature does not significantly affect the total mass transfer rate, although it produces an interesting entrance effect. Due to this fact, for design consideration, the solution inlet temperature may be set at equilibrium conditions for the given pressure and concentrations.
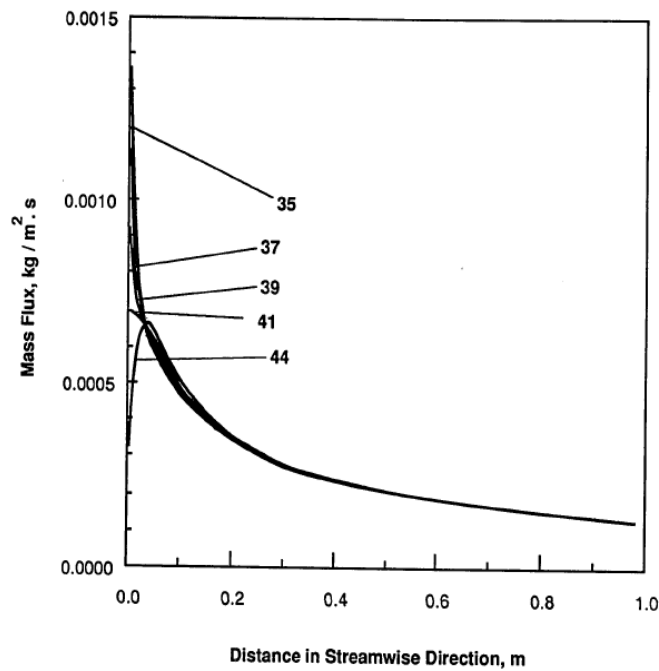

Fig. 11. Effect of the inlet film temperature on the absorbed mass flux at the interface

The mass absorbed at the interface is proportional to the absorber's length as illustrated in Figure 12. This process continues until the mass absorbed approaches an asymptotic value corresponding to the absorber pressure and the isothermal wall temperature near the end of the channel. This result supports the choice of the outlet conditions m (18).
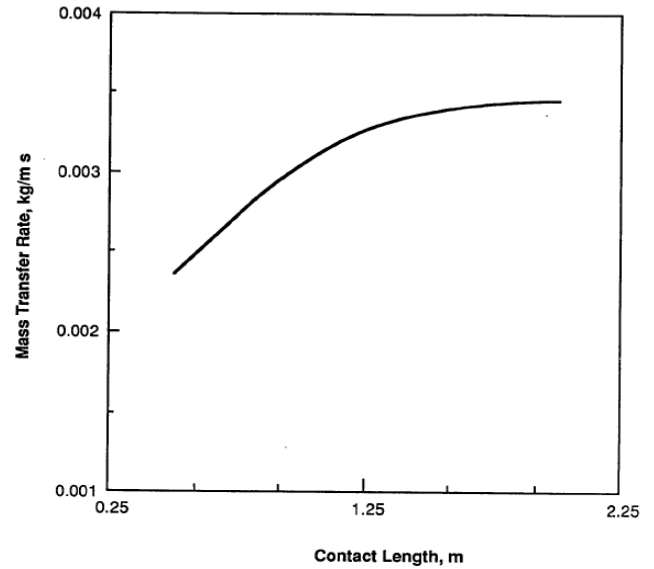
Fig. 12. Effect of contact length on absorption rate

Figure 13 shows a comparison of the concentration change in streamwise direction for LiBr with the experimental results of Kim [27]. The operating parameters are as the same listed in Table 1 except that absorber vapor pressure, 934.8 Pascal. The numerical solution shows similar trend as the experimental data.
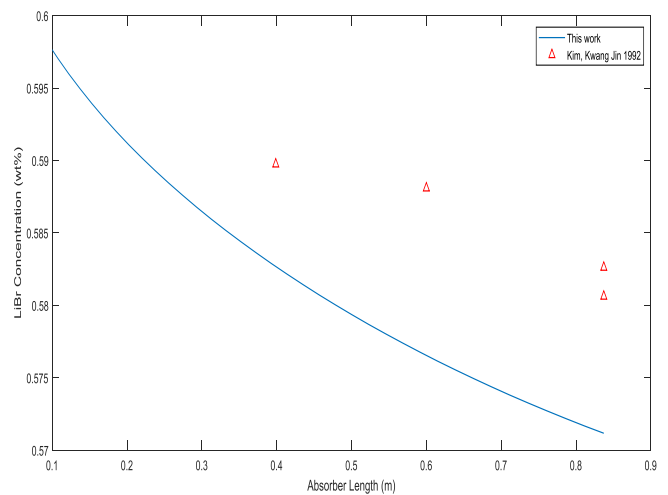
Fig. 13. Comparison of the average streamwise concentration

Figure 14 shows a comparison of the LiBr concentration change in streamwise direction for bulk and interface concentration with the numerical solution given by Andberg [6] for the same conditions as listed in Table 1. It is clear from the figure that there is a good agreement between these two studies.
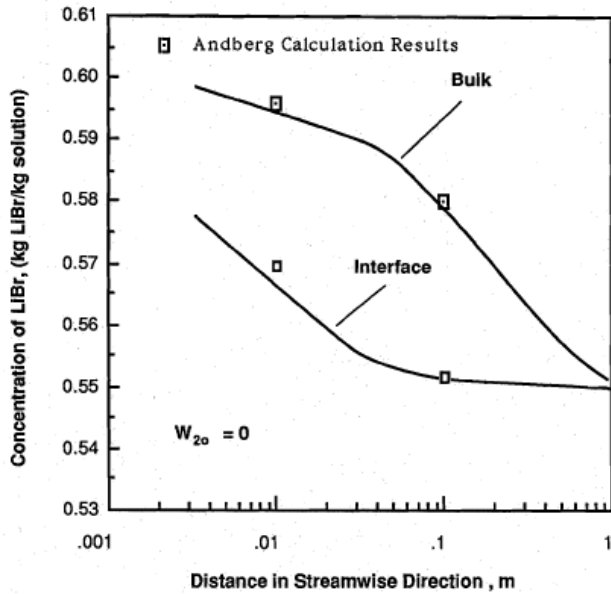
Fig. 14. Comparison of the average streamwise concentration

One disadvantage of the smooth film model is its inability to predict the effect of the film Reynolds numbers on the absorption process for (Re > 30). The experimental results of Yang [21] and Ameel [22] showed an increase in the absorption rate. This is basically due to presence of waves on the film surface for all Reynolds numbers.

CONCLUSION

In an effort to improve the modeling of the film absorption, a numerical model is presented which includes the governing equations for gas phase and shear stress at the interface. It was found that the absorption rate increases strongly by increasing the absorber water vapor pressure, the inlet solution concentration, or by lowering the isothermal wall temperature. The inlet solution temperature affects the entrance region only and has a limited effect on the absorption rate. From the analysis of the gas phase, part of the energy generated at the interface is transmitted to the gas phase and elevates its temperature.

One disadvantage of the smooth film model is its inability to predict the effect of film mass flow rate on the absorbed mass flux. Although the smooth film model is simple in analysis a lot of work has to be done to develop a reliable hydrodynamic theory for wavy film flow for better understanding the fundamental problem.

REFERENCES

[1] Nakoryakov V. E. and Grigor'eva N. I., "Combined heat and mass transfer during absorption in drops and films," Inzh.-Fiz. Zh., Vol. 32, 1977, 399-405.

[2] Grigor'eva N. I. and Nakoryakov V. E., "Exact solution of combined heat and mass transfer problem during film absorption," Inzh.-Fiz. Zh., Vol. 33, 1977, pp. 893-898.

[3] Nakoryakov V. E. and Grigor'eva N. I., "Calculation of heat and mass transfer in nonisothermal absorption on the initial portion of a downflowing film," Teore. Osn. Khim. Tek., Vol. 14, 1980, pp 483-488.

[4] Grossman G., "Simultaneous heat and mass transfer in film absorption under laminar flow," Int. J. Heat Mass Transfer, Vol. 26, 1983, pp. 357-371.

[5] Yih S. M., and Seagrave, "Mass Transfer in Laminar Falling Liquid Films with Accompanying heat transfer and Interfacial Shear," Int. J. Heat Mass Transfer, Vol. 23, 1980, pp. 749-758.

[6] Andberg J. W., "Non-isothermal absorption of gases into falling liquid films," 1982, M.S. Thesis, University of Texas at Austin, Austin, TX.

[7] Andberg J. W. and Vilet G. C., "Design guidelines for water LiBr absorbers," ASHRAE Transactions, Vol. 89, 1983, pp. 220-232.

[8] Yang R., and Wood B. D., "A Numerical Modeling of an Absorption Process on a Liquid Falling Film," Solar Energy, Vol. 48 No. 3, 1992, pp. 195-198.

[9] Conlisk A. T., "Falling film absorption on a cylindrical tube," AIChE J, Vol. 38, 1992; pp.1716-1728.

[10] Conlisk A. T., "Analytical solutions for the heat and mass transfer in a falling film absorber,"Chem Eng Sci., Vol. 50, 1995, pp. 651-660.

[11] Nakoryakov V. E., Grigor'eva N. I., and Potaturkina L. V., "Analysis of exact solutions to heat and masstransfer problems for absorption with films or streams," Theor. Found. Chem. Eng., Vol. 31, pp. 119–126.

[12] Nakoryakov V. E., Grigor'eva N. I., and Bartashevich M. V. , " Heat and mass transfer in the entrance region of the falling film: absorption, desorption, condensation and evaporation, " Int. J. Heat Mass Transf., Vol. 54, 2011, pp. 4485–4490.

[13] Yoon J. I., Phan T. T., Moon C. G., and Bansal P, "Numerical study on heat and mass transfer characteristic of plate absorber,"Appl Therm Eng., Vol. 25, 2005, pp. 2219-2235.

[14] Karami S., and Farhanieh B., "A numerical study on the absorption of water vapor into a film of aqueous LiBr falling along a vertical plate." Heat Mass Transf., Vol. 46, 2009, pp. 197-207.

[15] Bo S., Ma X., Lan Z. H., Chen J., and Chen H., "Numerical simulation on the falling film absorption process in a counter-flow absorber," Chem Eng J, Vol. 156, pp. 607-612.

[16] Meyer T., "Analytical solution for combined heat and mass transfer in laminar falling film absorption with uniform film velocity, isothermal and adiabatic wall," Int J Refrig, 2014, Vol. 48, pp.74-86.

[17] Meyer T., "Analytical solution for combined heat and mass transfer in laminar falling film absorption with uniform film velocity, adiabatic wall boundary," Int J Heat Mass Trans, Vol. 80, 2015, pp. 802-811.

[18] Mortazavi M., and Moghaddam S., "Laplace transform solution of conjugate heat and mass transfer in falling film absorption process," Int J Refrig, Vol. 66, 2016, pp. 93-104.

[19] Hosseinnia S. M., Naghashzadegan M., and Kouhikamali R., "Numerical study of falling film absorption process in a vertical tube absorber including Soret and Dufour effects," International Journal of Thermal Sciences, Vol. 114, 2017, pp. 123-138.

[20] Burdukov A.P., Bufetov, N.S., Deriy, N.P., Dorokhov, A. and Kazakov, V.I., "Experimental Study of the Absorption of Water Vapor by Thin Films of Aqueous Lithium Bromide," Heat Transfer-Soviet Rest, Vol. 12, 1980, pp. 118-123.

[21] Yang R., "Heat and mass transfer in laminar wavy film absorption with the presence of non-absorbable gases," 1987, Ph.D. Dissertation, Arizona State University, Tempe, AZ.

[22] Ameel T. A., "Non_absorbable gas effects on Heat and Mass Transfer in a falling film absorption," 1991, Ph.D. Dissertation, Arizona State. University, Tempe, AZ.

[23] Habib H. and Wood B. D., "Simultaneous Heat and Mass Transfer in Film Absorption with the Presence of Non-Absorbable Gases," J. Heat Transfer, Vol. 123 No. 5, 2000, pp. 984-989.

[24] Siebe D. A., "Evaluation of Air-Conditioning Systems Utilizing Liquid Absorbents Regenerated by Solar Energy," 1986, Ph.D. Dissertation, Arizona State University, Tempe, AZ.

[25] McNeely L. A., "Thermodynamic properties of aqueous solutions of lithium bromide," ASHRAE Transactions, Vol. 85, 1979, pp 413-434.

[26] Patankar S. V., "Numerical Heat Transfer and Fluid Flow," Hemisphere Publishing Corporation, 1980.

[27] Kim K. J., "Heat and mass transfer enhancement in absorption cooling," 1992, Ph.D. Dissertation, Arizona State. University, Tempe, AZ.

[28] Fulford G.D., "The Flow of Liquids in Thin Films " Adv, Chem. Eng., Vol. 5, 1964, pp. 151-235.